A real time affinity biosensor on an insulated polymer using electric impedance spectroscopy in dielectric microchips.

Mohammed Kechadi, Bruno Sotta, Lila Chaal, Bernard Tribollet, Jean Gamby

Real time affinity biosensor onto insulated polymer using electric impedance spectroscopy in dielectric microchip

Mohammed Kechadi,[a,b,c] **Bruno Sotta,**[d] **Lila Chaal,**[c] **Bernard Tribollet,** [a,b] **and Jean Gamby** [a,b,*]

This paper presents development real time monitoring of binding events onto flexible plastic in microchips. Two planar carbon microelectrodes are integrated into insulated polyethylene terephthalate microchip without direct electrical contact with the solution in microchannel. It has been possible to probe the electric impedance changes through the interface constituted by the microelectrode/ PET microchannel/ solution when a biomolecular interaction takes place onto the polymer surface. This new transduction for biosensing was demonstrated for the molecular recognition of BSA immobilized on the polymer microchannel surface using the corresponding rabbit anti-BSA antibodies as an analyte in the flow microchannel at the nanomolar range concentration. The equilibrium association constant was determined for the affinity reaction between both ligands and was obtained equal to $5\times10^7 M^{-1}$. The promising results obtained with this new device make it a competitive biosensor.

1 Introduction

The last decades have seen the emergence of microfluidic devices with various tranducers for affinity biosensor development. The most used tranducers are electrochemical [1],[2], electroacoustic [3],[4], or optical [5],[6] for detecting interactions between ligands. Surface plasmon resonance (SPR) is one of the most used optical biosensors for the measurement of the refractive index changes [7],[8]. As illustrated in Figure 1A with Biacore SPR instrument scheme, the ligand (antigen, receptor…) is immobilised in the hydrogel, while the analyte (antibody, messenger…) flows in the channel and diffuses in the gel where the ligand is bound. The metal/ dielectric interface constituted to glass slide coated with hydrogel and gold is excited by a beam of monochromatic light, in conditions of total reflection leading to the resonance. The light beam probes the hydrogel and detects changes in the local refractive index due to the accumulation of analyte mass. The depth of the evanescent wave is 100 nm towards the hydrogel, i.e. the thickness of the hydrogel itself.

In the last decades, several groups have focused on electrical signal transduction in microchip by using direct or indirect electrode configuration to measure the conductivity of the streaming electrolyte in microchannel. An original technique has been the development of measurements through capacitively coupled contactless conductivity detection (C^4D) through two electrodes with a distance separation constituting the detector cell [9],[10],[11]. However, the high applied ac voltage 0.5-10 V amplitudes are much larger than conventionally used values, 5 ~ 100 mV. Such large amplitude generates a non-linear relationship between voltage and current which cause distortion of impedance results. It is for this reason that this transduction can be viewed as pseudoimpedance or transimpedance technique.

In recent years, laser photoablation technique was used to defined a well-controlled microelectrodes position in polymer microchip. The feeble gap between the microelectrodes as well as with the thin layer of dielectric material that coated the microelectrode

allowed to avoid the linearity problem [12]. As mentioned for SPR, the principle of the developed electric impedance in dielectric microchip is also based on the metal/ dielectric interface excitation by applying a modulated voltage of one hundred of millivolts in frequency range through the dielectric layer. The output impedance through the device can thus be related to the interfacial impedance of the modified dielectric layer sandwiched between the microelectrodes and the flow microchannel (see Figure 1B). The crucial advantage of electric impedance spectroscopy on insulated polymer sandwiched between two microelectrodes is the absence of direct contact between the microelectrodes and the flow microchannel [12],[13]. As a consequence the polymer microchannel layer sandwiched between the two planar microelectrodes can be considered as a dielectric component [14] whose physical properties may change in response to an external electrical excitation. Based on this principle, in a previous paper, a flow sensor was developed to record at high fixed frequency the chemical conversion of enzymatic substrate like aminophenyl phosphate in PET microchannel through the channel resistivity [15]. In this paper, we demonstrate for the first time the possibility to probe the interfacial electric impedance change when a biomolecular interaction takes place between a ligand in solution (analyte) with a ligand attached onto the polymer microchannel. This new transduction for biosensing was demonstrated for the detection and quantification of bovine serum albumin (BSA) immobilized on the polymer microchannel surface using the corresponding rabbit anti-BSA antibodies (Ab-BSA) as an analyte, which is loaded in the flow microchannel at nanomolar range concentration. Experimental studies are based on the real time monitoring of the measured impedance variation at a fixed frequency (400 Hz) by applying a small 100 mV alternating potential excitation through two microband electrodes, during the association/ dissociation rate between Ab-BSA loaded in flow microchannel and BSA immobilized on PET.

2 Materials and methods

2.1 Chemicals

10 mM of Tris(hydroxymethyl)aminomethane (from Sigma Aldrich) was obtained after dilution in 10 mM HCl and 10 mM NaCl. The checked pH was at 9 and was used as the buffer solution. 1mM NaOH (from Sigma Aldrich) was used as washing buffer in a regenerating step. Bovine serum albumin (96%) was purchased from VWR International. The rabbit anti-bovine serum albumin antibodies (Ab-BSA) was received from Sigma-Aldrich. The antibody solutions were also diluted in the buffer solution from a 10^{-5} M Ab-BSA stock solution in 50% glycerol. Tween 20 solution was used with the ratio: Tween 20/buffer solution = 0.2 ml.L^{-1} [16].

2.2 Microchannel Networks

Photoablation procedure for the microchannel networks has been previously described [17],[12]. In brief, the microchip used in this work was realised by photoablation process which leads to the ablation of the material in contact with UV laser source. Before the photoablation step, the PET film thickness was measured at 100 µm. On the one side of the PET sheet two parallel microchannels (which will be transformed into microelectrodes) were drilled. The two microchannels depth into PET film was measured under microscope at 50 µm. On the other side of the PET sheet, a perpendicular microchannel for fluidic was drilled having a trapezoidal cross-section shape with a depth of 45 µm, a width of 100 µm and a length of 1.4 cm (See Figures 1B and C). Thus, a 5 µm thick PET layer separated the microchannel from the bottom of the two microelectrodes (See Figure 1B). The two parallels microchannels were transformed into microelectrodes by incorporation of a graphite carbon ink then dried afterward at 50°C. Finally the photo-ablated PET film was laminated using a 35 µm-PE/PET layer. As shown in Figures 1B and C, the distance separation between both microelectrodes is 120 µm edge to edge (200 µm center to center) and the detection surface area per microelectrode is 80 µm x 100 µm. Study was carried out by the electric impedance measurement in alternative mode (ac) through the two microelectrodes at frequency range from 1 MHz to 1 Hz with 0.1 V amplitude, in order to control the dielectrical behaviour of the overall microsystem and to extract the specific microchannel response from the background response [18].
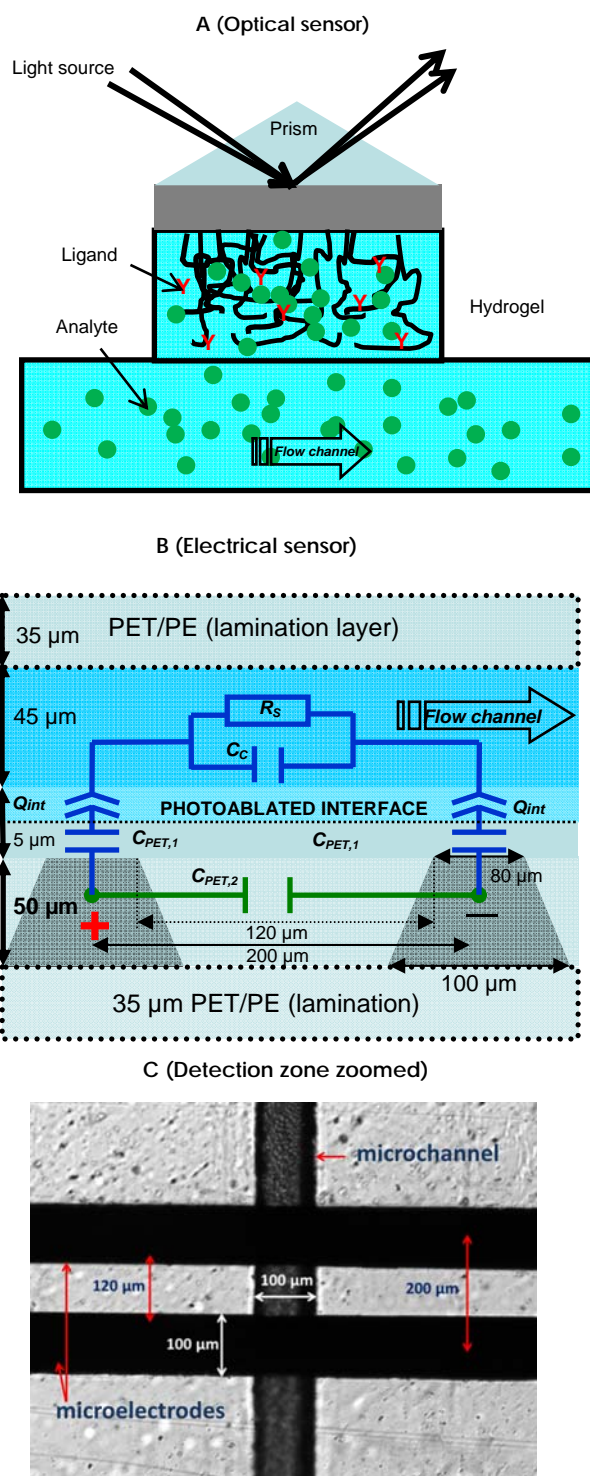

Figure 1. **A**. Schematic representation of the BIACORE optical biosensor. The hydrogel is 100 nm high approximately; the flow channel for a standard instrument is 24 mm long, 50 µm high and 500 µm width. The ligand is immobilised in the hydrogel, the analyte flows in the channel and diffuses in the gel where it binds to the ligand. **B**. Cross section of the dielectric interface microelectrode/ PET/ microchannel and the corresponding electrical equivalent circuit: $C_{PET,2}$ for the 120 µm-PET layer impedance (distance separation), $C_{PET,1}$ for the 5 µm-PET layer impedance (non-contact layer thickness), the element CPE, Q_{int}, for the interfacial impedance (photoablated surface), and the parallel association of the solution resistance, R_S, and the cell capacitance, C_C. Please note

that for a more detailed view of the interface the dimensions are not to scale. C. The zoomed detection is taken under an inverted microscope.

2.3 Instrumentation

Impedance measurements are performed using Dielectric interface (Solartron, DI 1260) gain phase impedance analyzer coupled with a frequency response analyzer (Solartron, FRA 1255). Dielectric interface is characterised by the large frequency range, from 1 mHz to 20 MHz. Software Smart (Solartron Analytical) was used as the computer control of all experimental set-up. Dielectric interface is usually used for high impedance measurement on high insulated material that is the case with polyethylene terephthalate. Indeed, current measurement range of the system varies from 6 mA to 100 fA, thus enabling measurement of very high impedance (100Ω to 100 TΩ). In this study, impedance measurement is making at low fixed-frequency (here 400 Hz) which was appropriate for sensing the interfacial impedance through the dielectric microchip device connected to a dielectric interface apparatus.

2.4 Experimental procedure for electric impedance measurements in dielectric microchip

The microchip characteristics with an insulated PET layer sandwiched between two galvanic isolated microelectrodes can be assimilated to a dielectric interface with, on the one part of the 5 μm-PET thin polymer layer, electronic charges on microelectrodes and, on the other part, ionic charges in the microchannel considering impedances for each part of the microchip (see Figure 1B).

The global impedance $Z_G(\omega)$ between the two microelectrodes with a filled microchannel depends on the different parts which constitute the microchip. In this configuration, $Z_G(\omega)$ can be expressed as the combination between $Z_1(\omega)$ (blue line in Figure 1B) and $Z_2(\omega)$ (green line in Figure 1B) [18], as expressed as follows,

$$Z_G(\omega)^{-1} = Z_1(\omega)^{-1} + Z_2(\omega)^{-1} \tag{1}$$

Firstly, acquisition and interpretation of electric impedance are performed with an empty microchannel through a 100 mV voltage excitation applied between the two carbon microelectrodes embedded in PET and separated to 200 μm center to center (120 μm edge to edge, Fig. 1B). The 120 μm-PET impedance layer, $Z_2(\omega)$, which separated two electrodes behaves as a capacitor (see equation 2) and will be eliminated from the global impedance, $Z_G(\omega)$, in further experiments when microchannel will be filled. The capacitance written in equation 2 was obtained at $C_{PET,2} = 8 \times 10^{-13}$ F.

$$Z_2(\omega) = \frac{1}{j\omega C_{PET,120\mu m}} \tag{2}$$

where ω is the angular frequency (rad s^{-1}), defined by $\omega = 2\pi f$, where f is the frequency.

The target application is the real-time monitoring of the electric impedance module variation $Z_1(\omega)$ at low frequencies. The latter impedance as appears in Figure 1B corresponds to a serial combination of three impedances as written below:

$$Z_1(\omega) = 2Z_{1,PET}(\omega) + 2Z_{int}(\omega) + Z_{microchannel}(\omega) \tag{3}$$

The first term in equation 3 is the 5μm-PET layer impedance from the top of one electrode to the channel bottom that behaves also as $C_{PET,120\mu m}$ (see equation 2). The value of $C_{PET,5\mu m}$ equals 14×10^{-11} F, is fixed and will be suppressed during the normalized procedure. The second term displayed in equation 3 is the microchannel solution impedance, Z_S, that corresponds to a parallel association between the microchannel solution resistivity, R_S, and the cell capacitance, C_C. The resistance R_S only depends on the buffer concentration that is high in comparison with the analyte concentration. The capacitance, C_C, is defined as a geometric capacitor that only depends on the chip dimension. This latter was equal to $C_C = 3 \times 10^{-13}$ F. The last term represents the interfacial impedance, Z_{int}, at the photoablated PET/ solution interface. As obtained in previous paper [19], this latter behaves as a non ideal capacitance represented by a constant phase element (CPE) where α_{int} and Q_{int} are the CPE exponent and the CPE element (see equation 4), respectively.

$$Z_{int}(\omega) = \frac{1}{(j\omega)^{\alpha_{int}} Q_{int}} \tag{4}$$

To conclude, Z_{int} is the only interesting parameter to monitor (see equation 3) which varies when a biomolecular interaction takes place on the photoablated PET surface throughout the course of the experiment. As a consequence, the real time monitoring of Z_{int} can be measured through the relative variation of Z_1. Indeed, this latter at low frequencies mainly reflects the contribution of the interfacial impedance as written in equation 5.

$$\Delta Z_1(\omega) = \Delta Z_{int} \tag{5}$$

2.5 Experimental procedure for adsorption monitoring

In the first step, PET microchannel was coated under a laminar flow contained 10^{-7} M BSA for 1200 s in order to saturate the microchannel surface. The solutions were loaded into the microchannel using high precise micropump with a flow rate equal to $F_v = 7.2$ μL min^{-1}. Indeed this optimized BSA concentration was chosen because it corresponds to the experimental plateau for BSA adsorbed onto PET surface [20]. Before loading the antibody, Tween 20 solution was also introduced over 1200 s to prevent the non specific adsorption of Ab-BSA in the molecular recognition step [16]. The molecular recognition step was the introduction of various Ab-BSA solution (from 10^{-8} to 10^{-7} M) in the same hydrodynamic conditions. The last step consisted in a washing procedure with 10^{-3} M NaOH for PET surface regeneration [20],[21],[22]. This procedure allows the start baseline recovering when water and the buffer solution were introduced again for a new started run experiment.

3. Results and discussion

3.1 Affinity reaction rate determination onto PET microchannel

A typical variation of the interfacial impedance module when Ab-

BSA solution is loaded on a prepared PET microchannel surface (BSA then Tween 20) is displayed in Figure 2. The initial value corresponds to the electric impedance module baseline obtained after BSA and Tween 20 samples were successively loaded in the microchannel (named Z_{BSA}). First, a control experiment was performed showing no significant changes on the measured interfacial impedance modulus when no rabbit anti-BSA antibodies are present in buffer solution (Figure 2, curve a). Secondly, the measured interfacial impedance modulus increases in the presence of Ab-BSA diluted with the buffer solution while the affinity reaction with BSA takes place. Then, the interfacial impedance signal response reaches a plateau value corresponding to a stationary signal (named Z_{Ab-BSA}). A statistical study about the changes on interfacial impedance modulus in presence of Ab-BSA is given in Table S1 (See the supplementary material).
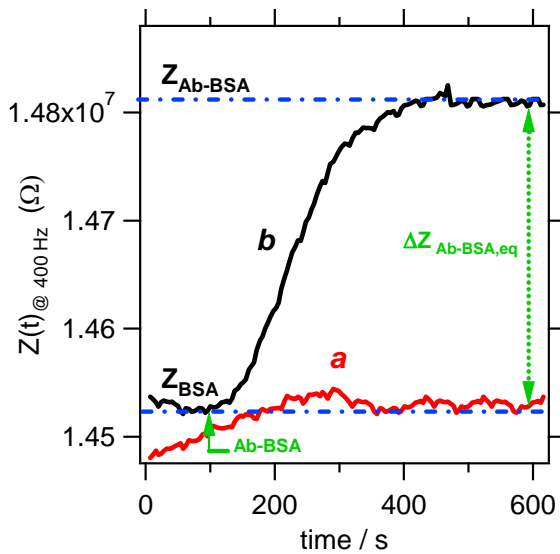

Figure 2. Sensorgrams showing the impedance module versus time. Curve a: A control experiment when no rabbit anti-BSA antibodies are present in buffer solution. Curve b: The association step between Ab-BSA as analyte and the adsorbed BSA on the microchannel sensor at a fixed frequency of 400 Hz and for a flow rate 7.2 µL.min⁻¹. Step 1: BSA and Tween 20 in buffer solution for microchannel coating. Step 2: Introduction of 4×10^{-8} M Ab-BSA diluted in the buffer solution.

The difference between the two stationary signals leads to an equilibrium status named $\Delta Z_{Ab-BSA,eq}$ which is equal to $Z_{BSA} - Z_{Ab-BSA}$. Plotting the equilibrium binding obtained from the difference values $\Delta Z_{Ab-BSA,eq}$ against various loaded Ab-BSA concentrations leads to an isotherm behaviour displayed in Figure 3A. Indeed, as the reaction binding progresses, the rate decreases gradually until a state that corresponds to an equilibrium between association and dissociation rates. The maximum value obtained for $\Delta Z_{Ab-BSA,eq}$ is more quickly reached while Ab-BSA concentration is high. We obtained a maximum value of $\Delta Z_{Ab-BSA,eq}$ (named $\Delta Z_{Ab-BSA,max}$) from a Ab-BSA concentration equals to 5×10^{-8} M. This means that all the active sites of BSA molecules adsorbed onto PET microchannel are saturated after the biomolecular recognition with Ab-BSA.

In order to find the model parameters corresponding to the binding reaction between Ab-BSA with BSA determined by impedance measurements, the relative equilibrium binding curve is plotted against Ab-BSA concentration after normalization of

$\Delta Z_{Ab-BSA,eq}$ values divided by $\Delta Z_{Ab-BSA,max}$ (displayed in the right-axis of Figure 3A). As described previously, for Ab-BSA concentrations lower than 5×10^{-8} M, the equilibrium binding varies linearly. The Langmuir equation model [23] has been tested to fit the experimental data synthetized in Figure 3 without good correlation. However, as yet known for heterogeneous sites for adsorption, the adapted Langmuir model named Langmuir-Freundlich model [20],[24],[25] was more adequate for the fitting procedure to determine the kinetics parameters.
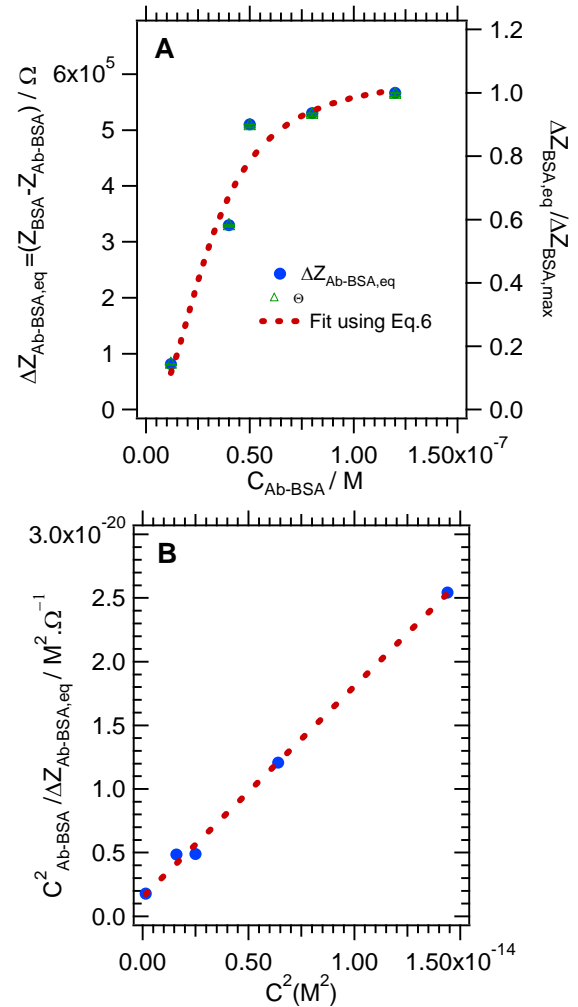
Figure 3. Calibration curve obtained for various Ab-BSA concentration loaded on the coated PET surface with BSA. (A) An association isotherm of Ab-BSA on the adsorbed BSA obtained from various experimental sensorgrams from 12 nM to 120 nM concentration. (B). Linearization step of the association isotherm using a linear fit as indicated in equation 7.

Briefly, in the described experiment, the impedance normalized in Figure 3b was assumed to be in linear correlation with the surface concentration of occupied sites. As a consequence, the Langmuir-Freundlich combined expression can be expressed as follows in equation 6 :

$$\theta\left(C_{Ab-BSA}{}^{m}\right) = \frac{\Delta Z_{Ab-BSA,eq}}{\Delta Z_{Ab-BSA,max}} = \frac{K^{app}_{BSA/Ab-BSA} C^{m}_{Ab-BSA}}{1+\left(K^{app}_{BSA/aAb-BSA} C^{m}_{Ab-BSA}\right)} \quad (6)$$

where θ (C^{m}_{Ab-BSA}) can be viewed as the capacity of the

microchannel to reach the maximum coverage, m exponent represents the power term of Freundlich, and the apparent equilibrium constant, $K^{app}_{BSA/Ab\text{-}BSA}$.

As traditionally admitted for the Langmuir equation[23], a linear expression of equation 6 is a useful test for the model validation as follows in equation 7:

$$\frac{C^m_{Ab-BSA}}{\Delta Z_{Ab-BSA,eq}} = \frac{1}{K^{app}_{BSA/Ab-BSA}\Delta Z_{Ab-BSA,\max}} + \frac{C^m_{Ab-BSA}}{\Delta Z_{Ab-BSA,\max}} \quad (7)$$

In order to obtain the traditional unit in M^{-1} for the equilibrium constant $K_{BSA/Ab\text{-}BSA}$ the following relation must be taking into account:
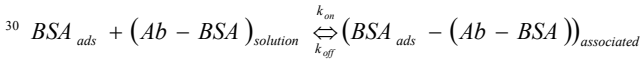
$$K^{app}_{BSA/Ab-BSA} = \frac{K_{BSA/Ab-BSA}}{[Ab-BSA]} \quad (8)$$

As predicted, a better fit of experimental data is obtained with the Langmuir-Freundlich equation and the obtained parameters are equal to $K^{app}_{BSA/\text{-}Ab\text{-}BSA} = 5\times10^{15}$ M^{-2} and $m = 2$. By replacing relation 8 in equations 6 and 7, we recover the typical Langmuir equation model with a power term corresponding to the unit ($m = 1$). The linearization step of the association isotherm using a linear fit as indicated in equation 7 leads to a straight line with a correlation coefficient R^2 equals to 0.996. Indeed, the curve fitting highlights a straight line characterized by a slope of 1.65×10^{-6} Ω^{-1} and an intercept of 1.51×10^{-21} $M^2.\Omega^{-1}$. From these values the parameters of equation 6 were obtained equal to $m = 2$, $\Delta Z_{Ab\text{-}BSA,max} = 0.606$ $M\Omega$ and $K^{app}_{BSA/\text{-}Ab\text{-}BSA} = 1.1\times10^{15}$ M^{-2}.

3.2 kinetic model for affinity reaction onto polymer microchannel

The interaction model for the binding reaction between Ab-BSA and BSA can be defined in the reaction scheme 1 below:

$$BSA_{ads} + (Ab - BSA)_{solution} \underset{k_{off}}{\overset{k_{on}}{\Longleftrightarrow}} (BSA_{ads} - (Ab - BSA))_{associated}$$

As demonstrated previously, results involve that the observed association rate, v_{obs}, between Ab-BSA and BSA can be expressed as a second order reaction proportional to the square of Ab-BSA concentration, as follows:

$$v_{obs} = k_{obs}[Ab - BSA]^2 \quad (9)$$

with v_{obs} in M s^{-1} and k_{obs} in M^{-1} s^{-1} represents the observed association kinetic rate constant.

Taking into account the concentration influence in the observed second order, the association kinetic rate constant can be determined as follows:

$$k_{on} = k_{obs}[Ab - BSA] \quad (10)$$

with k_{on} in s^{-1}.

The dissociation rate of BSA$_{ads}$-(Ab-BSA) complex, v_{off}, is proportional with the BSA$_{ads}$-(Ab-BSA) concentration and it is considered as a zero order reaction since the amount of the adsorbed complex BSA$_{ads}$-(Ab-BSA) onto PET microchannel can

be considered as a constant:

$$v_{off} = k_{off} \quad (11)$$

with k_{off} in M s^{-1} represents the dissociation kinetic rate constant As a consequence the ratio (k_{on}/k_{off}) is defined as the equilibrium constant, $K_{BSA/Ab\text{-}BSA}$ which is defined in M^{-1}.

The aim is now to determine by a full fitting procedure of the sensorgram impedance curve (see Figure 2), the kinetic parameters k_{on} and k_{off} leading to an estimation of the equilibrium constant of the complex BSA$_{ads}$-(Ab-BSA). For that, a theoretical expression of the impedance module $Z(t)$ at fixed frequencies with time can be written taking into account that the initial amount BSA adsorbed is related to impedance Z_{BSA} at the time $t=0$, as follows:

$$Z(t) - Z_{BSA} = \Delta Z_{Ab-BSA,\max}\left(\frac{k_{on}C_{Ab-BSA}}{k_{on}C_{Ab-BSA} + k_{off}}\right).\left[1 - \exp\left(-\left(k_{on}C_{Ab-BSA} + k_{off}\right)t\right)\right]$$
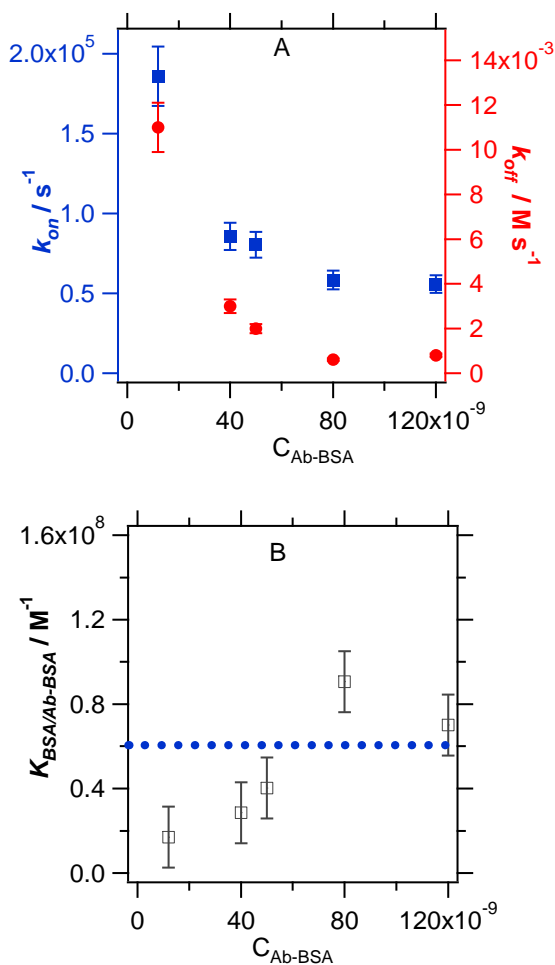
$$(12)$$

where $Z(t)$ in Ω is the impedance module measured at fixed frequency 400 Hz.
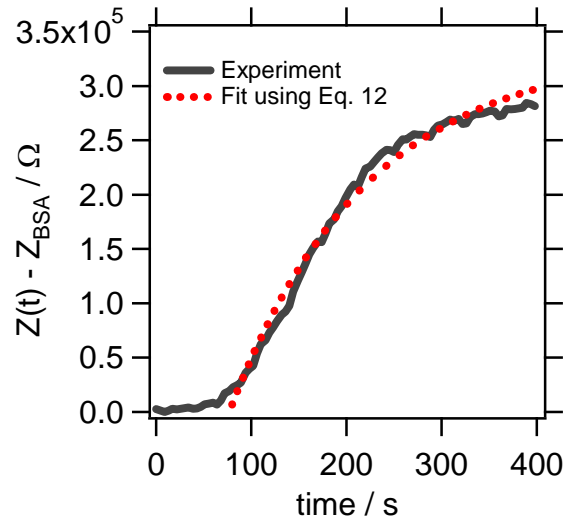
Figure 4. Experimental and fitted sensorgram of interfacial impedance modulus for 4×10^{-8} M of Ab-BSA loaded in the flow microchannel sensor showing the association reaction between Ab-BSA and the adsorbed BSA at a fixed frequency of 400 Hz and for a flow rate of 7.2 μL min^{-1}. The curve fit was performed with equation 12 leading k_{on}, k_{off} equal to 8.56×10^4 s^{-1} and 3×10^{-3} M s^{-1}, respectively.

The result of the fitting procedure using equation 12 is illustrated in figure 4 with a working Ab-BSA concentration taken at 4×10^{-8} M^{-1}. The obtained values of k_{on} and k_{off} are 8.56×10^4 s^{-1} and 3×10^{-3} M s^{-1} respectively. The same procedure was applied for various Ab-BSA concentrations and values of k_{on} and k_{off} have been determined for each curve (see Table S2 in the supplementary material). All the kinetic data obtained are synthetized in Figure 5A. It can be noticed that the values of k_{on} and k_{off} are slightly dependent on the Ab-BSA concentration while the ratio, k_{on} / k_{off}, is as expected, less dependent with Ab-BSA concentration, as appear in Figure 5B. This latter underlines that an average value for $K_{BSA/Ab\text{-}BSA}$ can be estimated at $(5.15\pm1.45)\times10^7$ M^{-1}, that is in

a good agreement with the literature [26]. It is observed that the average value is very close to the one obtained with the higher Ab-BSA concentration *i. e.* 1.2×10^7 M^1.

4. Concluding Remarks

15 Electric impedance spectroscopy in microchip was applied for the first time to monitor the biomolecular recognition of two ligands on insulated polymer designed as a microchip. As shown, the presence of BSA molecules immobilized onto the microchannel detection zone increases the interfacial impedance module 20 leading to a sensitive surface for biosensing in the nanomolar range concentration. The high sensitivity is found because this transduction takes advantage of the dielectric properties of the flow microchannel embedded in PET with two planar microband electrodes without contact with the solution, thus avoiding non 25 specific adsorption on microelectrodes and degradation of biological samples through uncontrolled faradic reactions.

Experimental results obtained highlight the possibility for the monitoring at low fixed-frequency of the electric impedance changes provoked by the association of proteic ligands. Here it is 30 illustrated for association reaction between rabbit anti-BSA antibodies in solution and BSA adsorbed onto the PET surface. Thus, it was found that the kinetics of association reaction rate depend on a second order kinetic law with the anti-BSA antibodies concentration. The promising results obtained for the 35 kinetic parameters and the equilibrium association constants between ligands using the present methodology make it a competing method for biosensing. The dielectric PET microchip is also a low cost and flexible material which offers a multiuse chip possibility. It could be used to screen putative partners in 40 biological fluids with regard to a specific protein. Also, the minute volumes of solvent used make it suitable as a detector for a capillary electrophoresis apparatus or to be connected with mass spectrometer.

Notes and references

50 *[a] CNRS, UMR 8235, Laboratoire Interface et Systèmes Electrochimiques, (LISE), F-75005 Paris, France .* Jean.gamby@upmc.fr*
[b] Sorbonne Universités, UPMC Univ Paris 06, UMR 8235, Laboratoire Interfaces et Systèmes Electrochimiques, (LISE), 4 Place Jussieu, F-75005, Paris, France.
55 *[c] Laboratoire d'Electrochimie, Corrosion et de Valorisation Energétique (LECVE), Faculté de Technologie, Université A. MIRA, Béjaia 06000, Algeria.*
[d] Sorbonne Universités, UPMC Univ Paris 06, UMR 7622, Laboratoire Biologie des Semences, 4 Place Jussieu, F-75005, Paris, France.
60

[1] A. Qureshi, Y. Gurbuz, S. Kallempudi and J. H. Niazi, *Physical Chemistry Chemical Physics* **2010**, *12*, 9176-9182.

[2] N. J. Ronkainen, H. B. Halsall and W. R. Heineman, *Chemical Society* 65 *Reviews* **2010**, *39*, 1747-1763.

[3] J. Gamby, M. Lazerges, C. Pernelle, H. Perrot, H. H. Girault and B. Tribollet, *Lab on a Chip* **2007**, *7*, 1607-1609.

[4] R. Schirhagl, U. Latif, D. Podlipna, H. Blumenstock and F. L. Dickert, *Anal. Chem. (Washington, DC, U. S.)* **2012**, *84*, 3908-3913.

70 [5] R. Davidsson, B. Johansson, V. Passoth, M. Bengtsson, T. Laurell and J. Emneus, *Lab on a Chip* **2004**, *4*, 488-494.

[6] F. B. Myers and L. P. Lee, *Lab on a Chip* **2008**, *8*, 2015-2031.

[7] J. Homola, *Analytical and Bioanalytical Chemistry* **2003**, *377*, 528-539.

75 [8] A. J. Tudos and R. B. M. Schasfoort in *Chapter 1 Introduction to Surface Plasmon Resonance, Vol.* The Royal Society of Chemistry, **2008**, pp. 1-14.

[9] A. J. Zemann, E. Schnell, D. Volgger and G. K. Bonn, *Analytical Chemistry* **1998**, *70*, 563-567.

80 [10] J. G. A. Brito-Neto, J. A. Fracassi da Silva, L. Blanes and C. L. do Lago, *Electroanalysis* **2005**, *17*, 1198-1206.

[11] J. Liu, J. Wang, Z. Chen, Y. Yu, X. Yang, X. Zhang, Z. Xu and C. Liu, *Lab on a Chip* **2011**, *11*, 969-973.

[12] J. Gamby, J.-P. Abid and H. H. Girault, *Journal of the American Chemical Society* **2005**, *127*, 13300-13304.

[13] J. Gamby, J. P. Abid, M. Abid, J. P. Ansermet and H. H. Girault, *Analytical Chemistry* **2006**, *78*, 5289-5295.

[14] G. Schaumburg, *Dielectrics Newsletter, Scientific Newsletter for Dielectric Spectroscopy* **1997**, *08*, 5-10.

[15] M. Faure, M. Kechadi, B. Sotta, J. Gamby and B. Tribollet, *Electroanalysis* **2013**, *25*, 1151-1158.

[16] J. S. Rossier and H. H. Girault, *Lab on a Chip* **2001**, *1*, 153-157.

[17] Z. Wu, H. Jensen, J. Gamby, X. Bai and H. H. Girault, *Lab on a Chip* **2004**, *4*, 512-515.

[18] M. Kechadi, J. Gamby, L. Chaal, H. Girault, B. Saidani and B. Tribollet, *Electrochimica Acta* **2013**, *105*, 7-14.

[19] M. Kechadi, J. Gamby, L. Chaal, B. Saidani and B. Tribollet, *Journal of Flow Chemistry* **2013**, *3*, 81-86.

[20] M. Kechadi, L. Chaal, B. Tribollet and J. Gamby, *Analyst* **2014**, *139*, 1492-1497.

[21] E. G. G. Spada, P. Giunchedi, *World Academy of Science, Engineering and Technology* **2011**, *52*, 245 249.

[22] V. Ferraro, R. F. Jorge, I. B. Cruz, P. M. L. Castro and M. E. Pintado, *J. Chem. Technol. Biotechnol.,* **2014**, 89, 671-681.

[23] I. Langmuir, *Journal of the American Chemical Society* **1918**, *40*, 1361-1403.

[24] E. A. James and D. D. Do, *Journal of Chromatography* **1991**, *542*, 19-28.

[25] G. P. Jeppu and T. P. Clement, *Journal of Contaminant Hydrology* **2012**, *129–130*, 46-53.

[26] A. Kausaite, M. van Dijk, J. Castrop, A. Ramanaviciene, J. P. Baltrus, J. Acaite and A. Ramanavicius, *Biochemistry and Molecular Biology Education* **2007**, *35*, 57-63.